applied sciences

MDPI

Article

Dissolved Organic Matter Behaviour by Conventional Treatments of a Drinking Water Plant: Controlling Its Changes with EEM-PARAFAC

Iván Sciscenko [1,*], Rita Binetti [2], Carlos Escudero-Oñate [3], Isabel Oller [4] and Antonio Arques [1]

[1] Departamento de Ingeniería Textil y Papelera, Universitat Politècnica de València (UPV), Plaza Ferrándiz y Carbonell s/n, 03801 Alcoy, Spain; aarques@txp.upv.es
[2] Centro Ricerche, Società Metropolitana Acque Torino S.p.A. (SMAT), 10127 Turin, Italy; rita.binetti@smatorino.it
[3] Institute for Energy Technology (IFE), Instituttveien 18, 2007 Lillestrøm, Norway; carlos.escudero@ife.no
[4] Plataforma Solar de Almería (PSA), CIEMAT, Ctra Senés km 4, Tabernas, 04200 Almería, Spain; isabel.oller@psa.es
* Correspondence: ivsci@txp.upv.es

Abstract: In the last 20 years, several articles related to the use of fluorescence excitation–emission matrices—parallel factor analysis (EEM-PARAFAC) to monitor dissolved organic matter (DOM) in drinking- and wastewater treatment plants were published. Noteworthy, its use in respective quality control laboratories remains scarce. To extend its popularisation, in this work, EEM-PARAFAC was employed to analyse the DOM composition changes along the different stages of the drinking water treatment plant administrated by *Società Metropolitana Acque Torino*. The best PARAFAC model was the one of three components, indicating that the Po River is constituted, mainly, by humic acid-like (HA-L) and tryptophan-like (Try-L) substances, the tyrosine-like ones being negligible (Tyr-L). Results indicated that physical treatments (sedimentation) did not produce a reduction in the PARAFAC scores; however, a 50% decay in 254 nm absorbance was observed. Fluorescent DOM was only removed with chemical treatments, obtaining ca. 70% HA-L scores decay with ozonation and 40% with chlorination. Furthermore, although ozonation degraded HA-L substances, the Try-L scores increased by 25%, indicating the transformation of HA-L into smaller molecules. On the contrary, total organic carbon measurements only exhibited a significant change when comparing the treatment plant's inlet and outlet (approximately a 45% decrease), but not within intermediate processes.

Keywords: chemometrics; chlorination; fluorescence spectroscopy; ozonation; quality control

Citation: Sciscenko, I.; Binetti, R.; Escudero-Oñate, C.; Oller, I.; Arques, A. Dissolved Organic Matter Behaviour by Conventional Treatments of a Drinking Water Plant: Controlling Its Changes with EEM-PARAFAC. *Appl. Sci.* **2024**, *14*, 2462. https://doi.org/10.3390/app14062462

Academic Editor: Dino Musmarra

Received: 1 February 2024
Revised: 8 March 2024
Accepted: 11 March 2024
Published: 14 March 2024

1. Introduction

Dissolved organic matter (DOM) consists of a complex mixture of derivatives of aromatic and aliphatic hydrocarbons, mainly humic substances, arising from soil and aquatic sources. Its composition is highly variable and depends on countless factors, such as its origin or agglomeration [1]. It has a remarkable influence on aqueous ecosystems, i.e., affecting the regulation of the nutrients' cycle or the microbial loop [2].

Within drinking water treatment plants (DWTPs), DOM monitoring is essential due to its many detrimental associated issues. For example, we can cite the generation of genotoxic and carcinogenic disinfection by-products (e.g., trihalomethanes or haloacetic acids) occurring after oxidation by the chlorination process [3], microorganism proliferation [4], or even membrane fouling enhancement [5], all of which result in an overall increase in water production costs.

Despite the paramount importance of DOM analysis, the most employed methods are based on non-specific measurements, such as non-purgeable organic carbon (NPOC) or ultraviolet absorbance at 254 nm (UVA). However, these methods provide partial information on the behaviour of the organic matter along the process [6]. Therefore, implementing

new analytical techniques able to provide deeper information on the composition of DOM whilst also being sensitive, fast, and easy to use, are necessary. In this sense, fluorescence spectroscopy meets all these requirements.

Excitation–emission matrices (EEMs) are three-dimensional plots of fluorescence intensity for each combination of excitation and emission wavelengths. The use of tridimensional data is an essential advantage of EEMs against UVA when studying samples with DOM from different sources, since the latter cannot differentiate between compounds with similar absorption spectra, while this might be possible if they differ in their fluorescence fingerprint [7].

Since typical fluorescence spectrometers could take between 10 and 40 min to acquire an EEM, the use of a single excitation wavelength is more practical for the real time monitoring. The most typical dimensionless values obtained from single emission spectra are the fluorescence index (FI), biological index (BIX), and humification index (HIX) [8–10]. Fortunately, due to the constant advancements in fluorescence spectrometers (as the replacement of the Xe lamp and monochromator for multiple single-wavelength LEDs as the excitation source [11]), the development of economic equipment for the instantaneous acquisition of EEMs is granted. This is important as FI, BIX, or HIX values have similar limitations as UVA, providing only background information compared to EEMs [12].

Traditionally, different types of DOM in an EEM were identified and quantified based on the visible peak-picking method [6,13]. Multivariate analysis methods, such as PARAFAC (parallel factor analysis), allow for the deconvolution of overlapping signals within an EEM, one being able to measure the individual fluorescence of the different DOM fractions on a set of samples, as well as elucidating their fingerprints [6,14,15]. Due to these reasons, PARAFAC is the most employed algorithm to analyse fluorescent organic matter within water treatment plants; the information about cases of application can be find elsewhere [16–18]. Currently, EEM-PARAFAC is still gaining momentum with its application with DOM real-time continuous monitoring [19–21], combination with machine learning [22,23], or even its detection of fluorescent emerging contaminants in wastewater effluents [24]. In this sense, our group has thoroughly explored, with success, the use of EEM-PARAFAC to visualise oxidative changes in fluoroquinolones (antibiotics), also being able to track the formation of fluorescent oxidation by-products and estimate its molecular structure [25–27].

Despite its gratifying progress, the real use of EEM-PARAFAC for DOM monitoring in DWTPs is still infrequent. Therefore, in this work, we have proposed to the facility that supplies drinking water to ca. 20% of Turin (Piedmont, Italy) inhabitants to apply this tool for the DOM monitoring along with the respective treatment lines. Its outcomes were compared with rutinary quality controls, NPOC and UVA, as well as with the FI, BIX, and HIX. The effects of the different treatment steps on the behaviour of the obtained scores for each PARAFAC-modelled component were evaluated in order to improve the efficiency of the treatments, as well as to adapt its application to tackle the recurring issue of seasonal algal blooms.

2. Materials and Methods

2.1. A Description of the Working Environment: The DWTP of Turin

Società Metropolitana Acque Torino (SMAT) is the company in charge of water cycle management in the Metropolitan Area of Turin. SMAT operates drinking, and wastewater, treatment plants, as well as the distribution networks in the area, supervising 291 municipalities and supplying a population of about 2.3 million inhabitants. The description of the treatment steps of the studied DWTPs reported in this work (shown in Figure 1) is below.

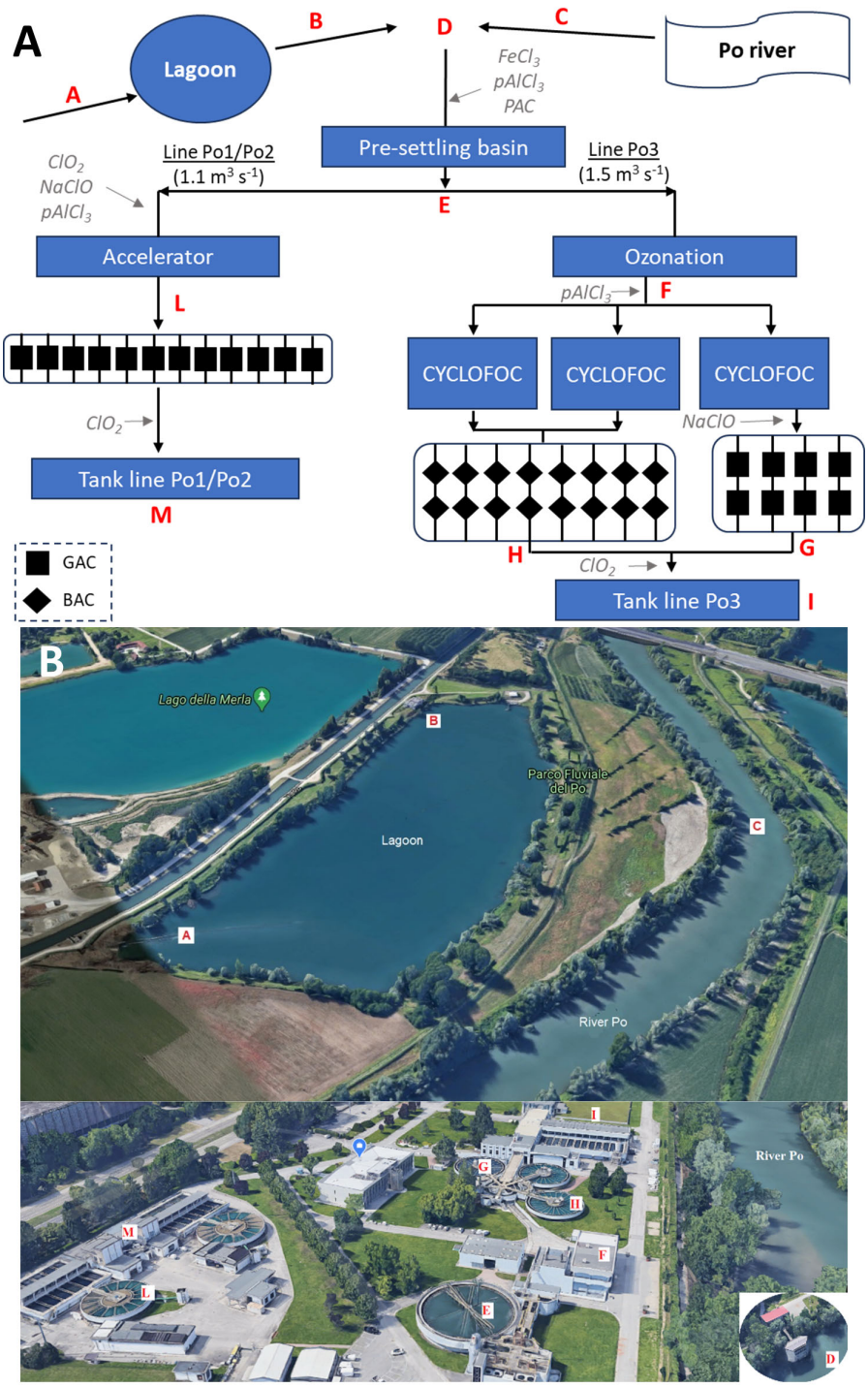

Figure 1. Sampling sites from SMAT DWTP, (**A**) scheme, (**B**) air pictures (taken from Map data ©2019 Google). Sampling sites are denoted with red colour letters.

The studied DWTP treats a mix of water from the river Po (site C) and a lagoon located about 10 km upstream (sites A and B, for the lagoon's inlet and outlet, respectively). The lagooning pre-treatment was included in the studied DWTP to improve the characteristics of treated water and reduce the amounts of chemical reagents needed along with the different processes. Water from sites B and C is mixed and passed through a wire mesh filter (6 mm^2 mesh size), which removes most of the coarse contaminants and sediments (site D) before flowing into the treatment plant. The river bed is pumped (ca. 3.6 m^3 s^{-1} flow) through 100 cm diameter steel pipelines into a static horizontal flow pre-settling basin (designed to handle a flow of 2 m^3 s^{-1}), which consists of a circular pool of 33 m

in diameter and 5.15 m high (4300 m^3 capacity and effective surface area of 850 m^2) and equipped with a rotary dredge for the mechanical removal of sludge, where additives (iron or aluminium chloride salts) are used to promote the sedimentation process. Powdered activated carbon (PAC) is also added to remove emerging contaminants in this step. The sludge, accumulated at the bottom, is evacuated by two electric pumps with a capacity of 35 L s^{-1}. At the outlet of the pre-settling basin (site E), the treatment plant is divided into three different lines, Po1 and Po2 (identical treatment lines hereafter named as Po1/Po2, with a total output of 1.1 m^3 s^{-1}) and Po3 (with an output of 1.5 m^3 s^{-1}).

For the two identical treatment lines, Po1/Po2, a pre-chlorination step takes place using chlorine dioxide (ClO_2, produced on-site by the combination of HCl and $NaClO_2$ with an output of 12 kg h^{-1} and conveyed to the various potabilisation system inlet points via PVC conduits) and sodium hypochlorite (NaClO, stored in fibreglass reinforced resin reservoirs and added to the treatment cycle by piston pumps via PVC pipes). Aluminium polychloride ($pAlCl_3$) flocculant is also administrated here with a capacity of 75–750 L^{-1} h^{-1}. Subsequently, the water is headed to the clarification step (site L), consisting of an "Accelerator" type sludge recirculation tank (diameter ca. 25 m, 1600 m^3 volume, and maximal output of 500 L s^{-1}). Finally, the treated water is filtered on 12 parallel lines units of granular activated carbon (GAC, filtering layer of 800 cm) and afterwards introduced into a tank where the final disinfection step with ClO_2 occurs (site M).

Regarding the other parallel line, Po3, the water undergoes an ozonation process (site F). O_3 is produced by four generators made up of 558 dielectric tubes with a production capacity of 8 kg h^{-1} each; the O_3 is blown into the water via porous ceramic plates arranged along the bottom of the contact chambers (a concentration of 1–2 mg L^{-1} of O_3 and a contact time of 5–10 min is finally reached). Right after ozonation, the water is transferred to three parallel CYCLOFOC clarifiers (where the precipitation of the sludge formed takes place promoted by the addition of $pAlCl_3$ and microsand) with an overall capacity of 1.5 m^3 s^{-1}. Each CYCLOFOC has a diameter of 24 m and a volume of 3150 m^3. At the outlet from one basin, a further oxidation treatment with NaClO takes place to eliminate NH_3 and related nitrogenated compounds, and afterwards, the water is passed through eight GAC filtration lines units (site G). To reduce the chlorinated disinfection by-products formation, the outlet from the other two CYCLOFOC basins is headed, instead, to 16 biological treatment units (BAC) (site H) and mixed with the ones from the chlorination process. G and H combination water is transferred to a tank where a final disinfection treatment with ClO_2 takes place in order to avoid the regrowth of bacterial colonies along with the distribution system during the delivery of the water to the final users (site I).

2.2. Sampling and Measurements

Samples from sites A to M were collected in dark glass vials (24 mL) with a Teflon septum and stored at 2–10 °C for up to 7 days before their analysis. pH changes between samples were negligible, exhibiting an average pH = 8.0 ± 0.3. Samples analysed by fluorescence spectroscopy were previously filtered through Chromafil Xtra PTFE 0.45 μm filters.

NPOC and dissolved organic carbon were determined using a Shimadzu TOC-V_{CPH} Total Organic Carbon Analyzer (Kyoto, Japan) equipped with a Shimadzu ASI-V autosampler (Kyoto, Japan). Prior to the analyses, samples were acidified with HCl 2 M (VWR Chemicals, Radnor, PA, USA) and sparged with ultra-pure carrier air to eliminate inorganic carbon. For dissolved organic carbon determinations, samples were previously filtered with 0.45 μm Whatman cellulose filters. However, since these values presented no significant differences with the NPOC ones, only the last ones are here reported. UVA was measured at 254 nm using a Hach Lange DR6000 spectrophotometer (Loveland, CO, USA). EEMs from both, samples and blanks, were recorded employing a Horiba PTI Quanta Master 400 spectrofluorometer (Kyoto, Japan); excitation range: 250–400 nm, and emission range: 300–600 nm (both recorded within 5 nm intervals).

2.3. FI, BIX, and HIX Calculation

The FI was calculated as the ratio between the emission intensity at 450 nm with that at 500 nm when employing an excitation wavelength of 370 nm [28]. The BIX was calculated as the ratio between fluorescence intensities from the emission spectrum at 380 and 430 nm, respectively, excited at 310 nm [29]. Finally, the HIX was calculated as the ratio of the 435–480 nm emission spectrum with the analogous one of 300–345 nm (excitation wavelength 254 nm) [30].

2.4. EEM-PARAFAC Model

The PARAFAC analysis was performed employing MATLAB2018b, with a free graphical user interface based on the drEEM toolbox, EEMlab [31]. The dataset consisted of 88 EEMs, 6 blanks, and 6 Raman scans. Due to the low absorbance of the samples, the inner filter effect correction was not considered (the samples' absorbance within the range 250–600 nm were always below 0.05). Intensity standardisation was carried out by using the water Raman scatter peak at 350 nm excitation wavelength [32]. The modelling methodology was analogous to that of previous works [26,33]: (i) scattering was corrected (first-order Rayleigh scattering was eliminated with missing values, whereas second-order Rayleigh and Raman first- and second-order scattering were corrected by interpolation, respectively) and outliers were detected and eliminated (mostly EEMs from I site due to their negligible fluorescence); (ii) EEMs were normalised to their total signal to give the same leverage to each fluorophore; (iii) an exploratory modelling was carried out, observing that the model of three components was the one that, tentatively, could better describe the dataset; (iv) the model obtained was refined and afterwards validated based on the core consistency diagnostic (CORCONDIA) and split-half analysis [23,34]; (v) normalisation was reversed to obtain the scores corresponding to each component from the respective EEM on the dataset.

3. Results and Discussion

3.1. UVA and NPOC Measurements

UVA and NPOC are indicators of total DOM content in each sampling site, without giving information about their origin or class [26]. As expected, inlet sites exhibited greater UVA and NPOC values than the outlet ones (see Figures 2A and 2B, respectively). In this sense, site D (DWTP's inlet) had a UVA of 4 ± 1 m^{-1}, being of 1.0 ± 0.4 m^{-1} at the end of treatment line Po1/Po2 in site M (ca. 75% absorbance decay), and of 0.38 ± 0.02 m^{-1} after treatment line Po3 in site I (ca. 90% absorbance decay). On the other hand, NPOC results showed an average value around 1250 μg L^{-1}, only observing a reduction of 40–50%, approximately, at the final effluent from each treatment line, being of $(6.6 \pm 0.9) \times 10^2$ μg L^{-1} at the site I, and $(7.8 \pm 0.7) \times 10^2$ μg L^{-1} at site M. This indicates that organic matter separation is through sedimentation/filtration processes or oxidation/mineralisation in the case of chemical treatments. In addition, it can also be observed that: (i) sites A to D showed analogous UVA values, whereas the NPOC indicated that site B had slightly less organic matter content than A and C, site D having the average between B and C as expected; (ii) the sedimentation (and adsorption by PAC) step reduces influent UVA (site E = 1.8 ± 0.5 m^{-1}), but the NPOC remains unchanged; and (iii) analogous DOM degradation efficiency by BAC and chlorination as similar UVA values were obtained in sites H (1.2 ± 0.6 m^{-1}) and G (1.5 ± 0.5 m^{-1}), respectively.

3.2. Fluorescence Results

3.2.1. Fluorescence, Biological, and Humification Indexes

In order to obtain a quick overview of the behaviour of fluorescent DOM in the DWTP, a set of three indexes was calculated: the fluorescent index (FI), biological index (BIX), and humification index (HIX), results shown in Figure 3.

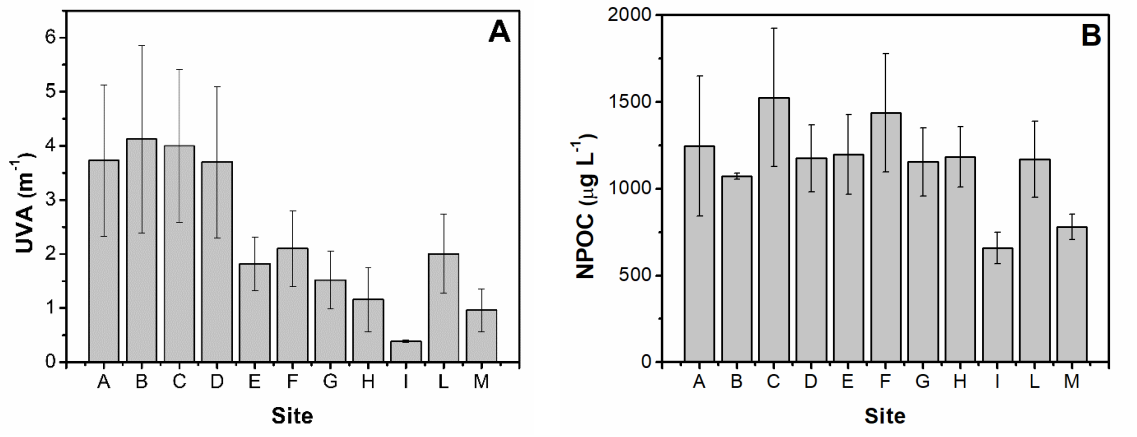

Figure 2. Obtained values in each sampling point for: (**A**) UVA; (**B**) NPOC. Values represent the average of consecutive measurements and error bars the associated uncertainty.

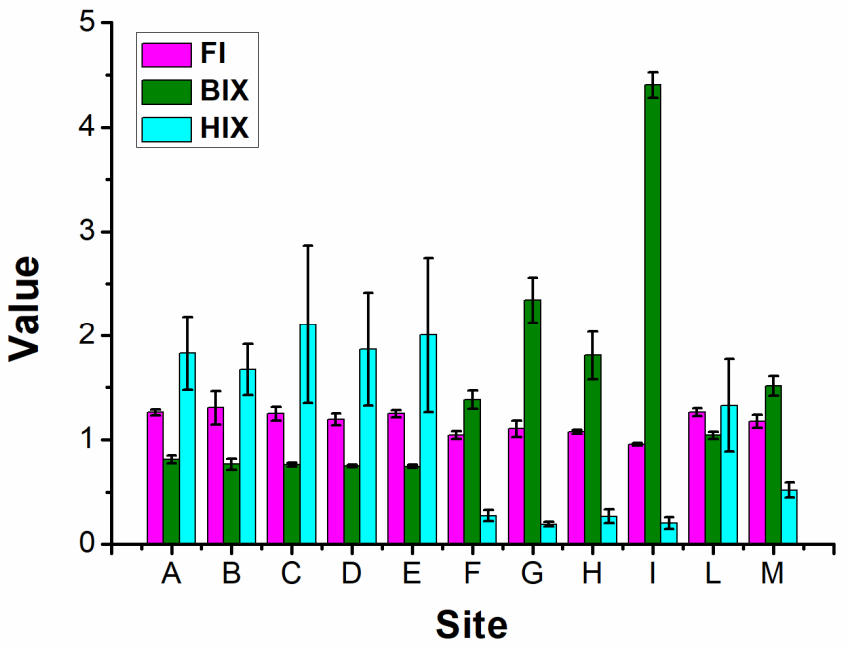

Figure 3. Fluorescence background analysis: FI, BIX, and HIX values per site.

By calculating the FI from the lagoon inlet and outlet (sites A and B, respectively), Po River's raw water (site C), and the inlet to the DWTP (site D, mixture of sites B and C), the FI is in all cases below 1.4, indicating that DOM sources are mostly terrestrial [28]. The FI values remained practically constant along the whole DWTP, indicating that it is not a sensitive parameter to analyse the aforementioned processes, although useful to rapidly characterise the raw water at the inlet points (sites A to D).

The BIX of inlet sites is approximately 0.8, which indicates an intermediate autochthonous component on DOM sources [8,29]. The BIX drastically changed from the inlet points (sites A to D, where it was practically constant as mentioned before) to the ones that suffered a chemical/biological process (treatment lines Po1/Po2 and Po3). In fact, BIX values are inversely proportional to those obtained by UVA and NPOC (discussed above) and EEM-PARAFAC (*vide infra*), being much higher at those where a chemical (ozonation or chlorination) or biological process was applied. Although, in this case, it is clearly not related with the presence of β fluorophore (characteristic of autochthonous biological activity), due to its definition, the obtained results indicated that a degradation process produces an increment on a 380 nm emission signal and/or a reduction in the 430 nm one, which is in line with the expected reduction in the double bond conjugation

and production of smaller molecules (i.e., fluorescence shift to shorter excitation–emission wavelengths or blue-shift) [35].

In line with the results from the BIX, the HIX was negligible after the ozonation process (site F) but considerable after chlorination (site L). It is worth mentioning that a decrease in the HIX is correlated with a decrease in acute toxicity along water treatment plants [10].

3.2.2. PARAFAC Model

Three models were explored in this EEM-PARAFAC analysis, decomposing the EEM into two, three, and four components, respectively. According to CORCONDIA results (Table 1), the model which best fitted the data was the one with three components, since an abrupt decrease in the core consistency was observed between the three- and four-component model. When performing the split-half analysis, this model was validated with a 0.95 Tucker's correlation coefficient. Residuals were also distributed randomly (Table 2).

Table 1. CORCONDIA obtained results for each tested PARAFAC model.

Number of Components	CORCONDIA (%)
2	92.5
3	98.0
4	11.7

Table 2. Measured, modelled, and residuals from some example sampling points obtained for the three−component PARAFAC model.

Site	Measured EEM	Modelled EEM	Residual
D	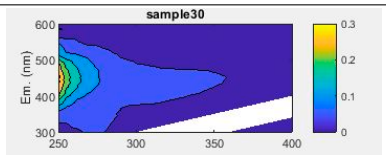	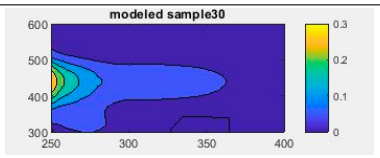	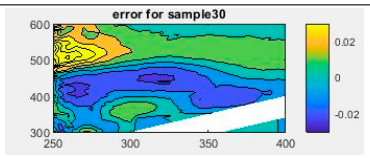
E	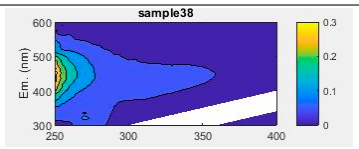	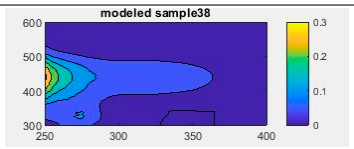	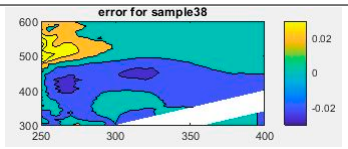
F	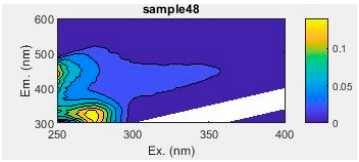	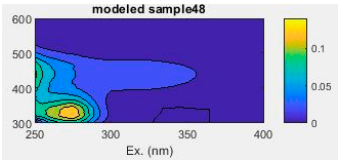	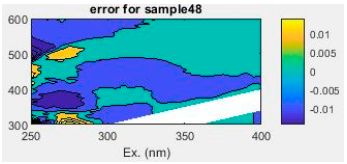
G	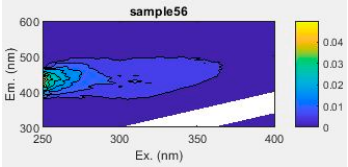	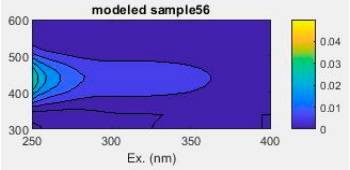	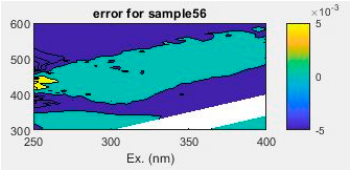
H	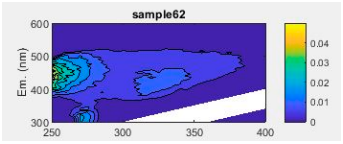	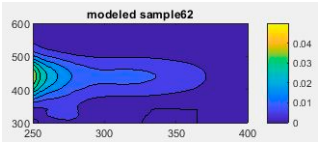	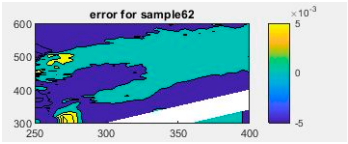

Table 2. *Cont.*

Site	Measured EEM	Modelled EEM	Residual
L	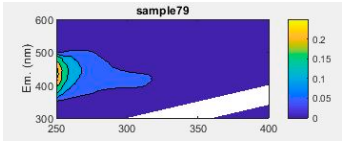	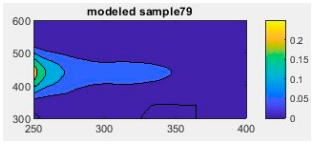	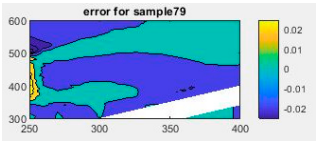
M	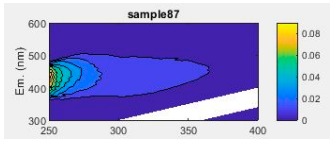	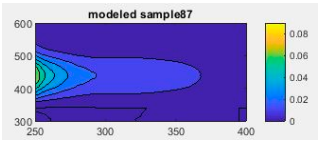	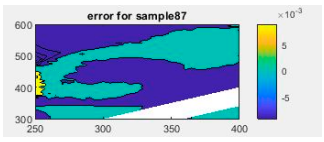

The three components' fingerprints can be found in Figure 4. According to their excitation and emission maxima, the PARAFAC components can be characterised as follows: deconvoluted component number 1 (X1), with a maximum < 250 nm excitation axis and ca. 440 nm emission axis that could be associated with either terrestrial humic or humic acid-like substances (HA-L). X2 with its maximum at 270/330 nm excitation/emission coordenates could be assigned to tryptophan-like substances (Try-L). Finally, X3, with its maximum at <250/300 nm, can most likely be associated with tyrosine-like substances (Tyr-L) [17,36]. In this sense, X2 could be considered the most relevant component regarding quality assurance monitoring, as it is reported that Try-L are potential indicators of *Escherichia coli* presence, whereas algal organic matter is associated with X1 [37,38].

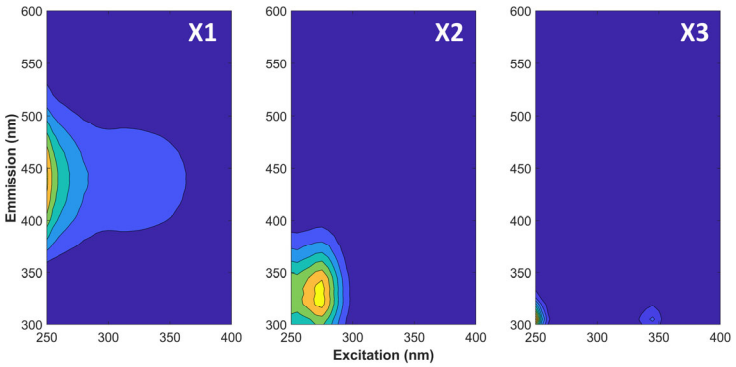

Figure 4. Fingerprints from the three-component PARAFAC model: X1 (HA-L), X2 (Try-L), and X3 (Tyr-L).

3.2.3. DOM Characterisation

As shown in Figure 5, when analysing the score values from each modelled component, the HA-L (X1) and Try-L (X2) have significant fluorescence signals along with the whole dataset, whereas Tyr-L (X3) score values were negligible in all cases, only detected at the outlet of both treatment lines (sites I and M). It is important to highlight that score values cannot be related directly to the abundance of each chromophore, as the fluorescence emission is not only dependent on the concentration but also on its quantum yield, which is characteristic of each chromophore.

In the lagoon inlet (site A), HA-L had a lower fluorescence signal than at the outlet (site B), and the same was observed for the Try-L ones. The influents had score values of 2.1 ± 0.2 of HA-L and 0.42 ± 0.02 of Try-L, respectively, and after the lagooning process, they increased to 3.2 ± 0.6 of HA-L and 0.83 ± 0.09 of Try-L. These observations might be attributed to organic matter derived from algae growth or the biodegradation of protein-like substances, whose by-products emit as HA-L and Try-L, resulting in an overall fluorescence increment for these two [39]. Comparable levels of these types of DOM were detected in raw river water (site C), being 2.6 ± 0.3 and 0.60 ± 0.06 for HA-L and Try-L, respectively.

The characterisation of DOM is in line with that observed from the FI and BIX values (Figure 3). As expected, in the spot where the lagoon outlet and Po River are mixed (site D), the HA-L and Try-L scores were the average between the ones from sites B and C, being 2.9 ± 0.3 for HA-L and 0.63 ± 0.04 for Try-L, in line with NPOC results (Figure 2B).

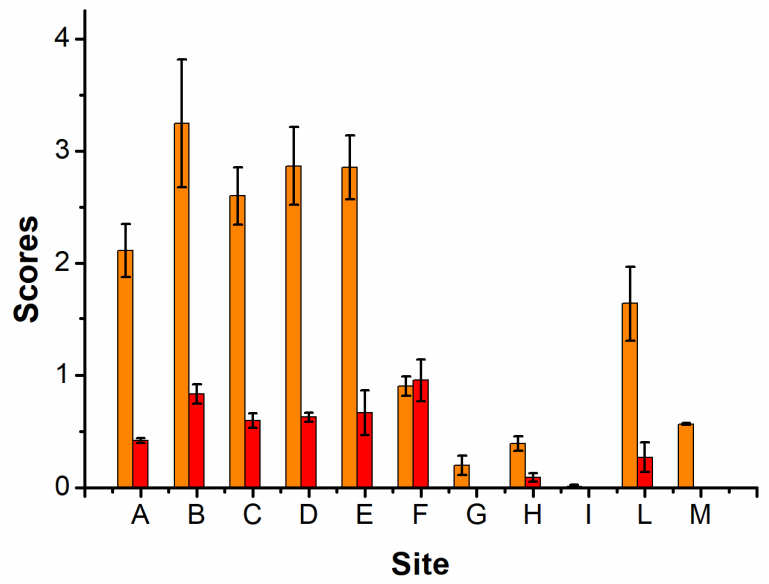

Figure 5. Results from fluorescence spectroscopy: PARAFAC components' evolution along the DWTP: X1 (orange), X2 (red), and X3 (pink, not observable).

3.2.4. Effect of Water Treatments

At the outlet of the pre-settling basin (site E), HA-L and Try-L scores remained constant with respect to site D, indicating the negligible effect of $FeCl_3$, $pAlCl_3$, or PAC on fluorescent DOM. However, regarding total DOM, from site D to E, an UVA reduction of 51 ± 32% was observed (Figure 2A), thus indicating colloidal organic matter and/or only the non-fluorescent DOM is removed by sedimentation process, which is in line with the observations reported by other authors [40,41].

Regarding line Po3, in the samples from the ozonation treatment (site F), a 68% reduction in HA-L score values was observed compared to site E, indicating that O_3 is efficient to remove these types of substances. Contrarily, Try-L scores exhibited a 25% increment compared to site E. Therefore, HA-L oxidation by-products might be similar molecular structure to (or emit in the same region as) Try-L substances, in agreement with an aromatisation decay of DOM, reflected on the observed excitation–emission blue shift [35], which is in line with the BIX results (see Figure 3). The latter blue-shift was not observed with the chlorination process applied at the exit of one of the CYCLOFOC basins (site G), where an overall decay of both PARAFAC components scores was observed (Try-L scores being negligible). Although slightly higher than after the chlorination process, very low score values were also observed at site H (approximately 0.4 and 0.1 for HA-L and Try-L, respectively), in line with UVA results (Figure 2A), indicating that more hazardous NaClO use might be replaced by BAC if the DWTP is re-designed. The treatment line's outlet (site I, which concerns water ready for distribution to the city network and consumption) effectively had negligible levels of fluorescent DOM.

On the other hand, analysing line Po1/Po2, the water coming from site E to site L (treatment with NaClO and ClO_2), the score values from HA-L and Try-L decayed 43 and 59%, respectively. Interestingly, when comparing these results with the ones from the ozonation in line Po3, the set of by-products was clearly different: whereas for ozonation a plausible transformation from HA-L to Try-L was observed, in samples obtained from site L, an indistinct decrease for both components was evidenced. These results can be explained by taking into account that ClO_2/ClO^- are less selective than O_3, which normally shows a

clear preference towards double bonds [42,43], thus favouring the conversion of HA-L into Tyr-L. At the final stage of this treatment line (site M), the outflow had negligible levels of Try-L substances but considerable for HA-L ones (0.566 ± 0.008), contrary to the treatment line Po3's final outflow (site I).

4. Conclusions

EEM-PARAFAC was successfully applied to track and characterise DOM at almost trace levels along the DWTP of Turin, Italy, providing information about the types of DOM and plausible chemical reactions happening along the DWTP. Even though NPOC and UVA are useful methodologies in DWTPs to rapidly check the DOM behaviour along the plant, only EEM-PARAFAC was able to properly track the trends of the different types of DOM and provided deeper layers of information regarding chemical changes. NPOC was the less sensitive technique, and changes were only observed when comparing the inlet and the outlet of each treatment line (D vs. I and M, respectively). When comparing EEM-PARAFAC with the FI, BIX, and HIX, although the indexes might offer a rapid on-line monitoring of fluorescent DOM, they do not differentiate HA-L substances from Try-L ones. Nevertheless, the BIX was shown to be a sensitive parameter to analyse fluorescence blue-shift due to decay on conjugated double bonds as a result of oxidative processes.

In terms of processes' efficiency, the lagooning pre-treatment did not produce significant water quality improvement (site A vs. B) in terms of DOM content. Measurements of emerging contaminants by high-resolution mass spectroscopy will be required to better understand its usefulness. Differences between fluorescent and non-fluorescent DOM were observed when comparing the effect of flocculation and sedimentation (from sites D to E), since only a reduction in UVA was observed, HA-L and Try-L scores remained without significant changes. Chlorination and ozonation oxidise DOM into smaller molecules, although the first might lead to the formation of chlorinated disinfection by-products. The use of BAC was shown to reduce HA-L/Try-L content in a similar way as NaClO, the former being evidently safer.

In future studies, we expect to analyse the reproducibility of works reporting that DOM monitoring by EEM-PARAFAC is a useful tool to predict emerging contaminants (e.g., pharmaceuticals) degradation or chlorinated disinfection by-products formation. The water treatment field certainly needs more studies to prove the reproducibility of these statements, as it will mean that extremely valuable information could be extracted from a simple and economic methodology. Furthermore, measuring DOM content at different stages of the year could be useful towards algae proliferation evaluations (one of the most challenging issues in DWTPs).

Author Contributions: Conceptualisation, A.A. and R.B.; methodology, I.S.; software, I.S.; formal analysis, I.S.; investigation, I.S.; resources, A.A., I.O., C.E.-O. and R.B.; writing—original draft preparation, I.S.; writing—review and editing, A.A., I.O., C.E.-O. and R.B.; supervision, A.A. and R.B.; project administration, A.A, I.O., C.E.-O. and R.B. All authors have read and agreed to the published version of the manuscript.

Funding: The authors want to acknowledge the financial support of Spanish Ministry of Science and Innovation (MCI) for funding under the AquaEnAgri Project (Reference: PID2021-126400OB-C31). I. Sciscenko also acknowledges the financial support of Generalitat Valenciana (CIAPOS/2021/311, project SANITISE).

Institutional Review Board Statement: Not applicable.

Informed Consent Statement: Not applicable.

Data Availability Statement: The raw data supporting the conclusions of this article will be made available by the authors on request.

Acknowledgments: The authors want to thank Dimitra Papagiannaki for the sampling and dedication devoted to finish this work at SMAT.

Conflicts of Interest: Author Rita Binetti was employed by the company Società Metropolitana Acque Torino S.p.A. (SMAT). The remaining authors declare that the research was conducted in the absence of any commercial or financial relationships that could be construed as a potential conflict of interest.

References

1. Leenheer, J.A.; Croué, J.P. Characterizing Aquatic Dissolved Organic Matter. *Environ. Sci. Technol.* **2003**, *37*, 18A–26A. [CrossRef]
2. Mostofa, K.M.G.; Liu, C.; Mottaleb, M.A.; Wan, G.; Ogawa, H.; Vione, D.; Yoshioka, T.; Wu, F. Dissolved Organic Matter in Natural Waters. In *Biogeochemistry*; Mostofa, K.M.G., Yoshioka, T., Mottaleb, A., Vione, D., Eds.; Environmental Science and Engineering; Springer: Berlin/Heidelberg, Germany, 2013; Volume 179, pp. 1–137. ISBN 978-3-642-32222-8.
3. Miklos, D.B.; Wang, W.L.; Linden, K.G.; Drewes, J.E.; Hübner, U. Comparison of UV-AOPs (UV/H2O2, UV/PDS and UV/Chlorine) for TOrC Removal from Municipal Wastewater Effluent and Optical Surrogate Model Evaluation. *Chem. Eng. J.* **2019**, *362*, 537–547. [CrossRef]
4. Osman, R.M.; Hodaifa, G. An Overview of Anaerobic Membrane Bioreactors: Current Developments, Fouling Problems, and Future Prospects. *J. Environ. Chem. Eng.* **2023**, *11*, 111482. [CrossRef]
5. Stein, N.; Sharon-Gojman, R.; Mauter, M.S.; Bernstein, R.; Herzberg, M. Fouling of Reverse Osmosis Membrane with Effluent Organic Matter: Componential Role of Hydrophobicity. *ACS ES T Water* **2023**, *3*, 2491–2501. [CrossRef]
6. Li, L.; Wang, Y.; Zhang, W.; Yu, S.; Wang, X.; Gao, N. New Advances in Fluorescence Excitation-Emission Matrix Spectroscopy for the Characterization of Dissolved Organic Matter in Drinking Water Treatment: A Review. *Chem. Eng. J.* **2020**, *381*, 122676. [CrossRef]
7. Sgroi, M.; Anumol, T.; Roccaro, P.; Vagliasindi, F.G.A.; Snyder, S.A. Modeling Emerging Contaminants Breakthrough in Packed Bed Adsorption Columns by UV Absorbance and Fluorescing Components of Dissolved Organic Matter. *Water Res.* **2018**, *145*, 667–677. [CrossRef]
8. Sururi, M.R.; Dirgawati, M.; Notodarmojo, S.; Roosmini, D.; Putra, P.S.; Rahman, A.D.; Wiguna, C.C. Chromophoric Dissolved Organic Compounds in Urban Watershed and Conventional Water Treatment Process: Evidence from Fluorescence Spectroscopy and PARAFAC. *Environ. Sci. Pollut. Res.* **2023**, *30*, 37248–37262. [CrossRef] [PubMed]
9. Lin, Y.; Hu, E.; Sun, C.; Li, M.; Gao, L.; Fan, L. Using Fluorescence Index (FI) of Dissolved Organic Matter (DOM) to Identify Non-Point Source Pollution: The Difference in FI between Soil Extracts and Wastewater Reveals the Principle. *Sci. Total Environ.* **2023**, *862*, 160848. [CrossRef]
10. Zhang, B.; Shan, C.; Hao, Z.; Liu, J.; Wu, B.; Pan, B. Transformation of Dissolved Organic Matter during Full-Scale Treatment of Integrated Chemical Wastewater: Molecular Composition Correlated with Spectral Indexes and Acute Toxicity. *Water Res.* **2019**, *157*, 472–482. [CrossRef]
11. Ferguson, T.; Bernicky, A.; Kozin, I.; Loock, H.-P. HPLC-Detector Based on Hadamard-Transform Fluorescence Excitation-Emission-Matrix Spectroscopy. *Anal. Chem.* **2021**, *93*, 8116–8121. [CrossRef]
12. Yang, L.; Hur, J. Critical Evaluation of Spectroscopic Indices for Organic Matter Source Tracing via End Member Mixing Analysis Based on Two Contrasting Sources. *Water Res.* **2014**, *59*, 80–89. [CrossRef] [PubMed]
13. Coble, P.G. Characterization of Marine and Terrestrial DOM in Seawater Using Excitation-Emission Matrix Spectroscopy. *Mar. Chem.* **1996**, *51*, 325–346. [CrossRef]
14. Peleato, N.M.; Legge, R.L.; Andrews, R.C. Neural Networks for Dimensionality Reduction of Fluorescence Spectra and Prediction of Drinking Water Disinfection By-Products. *Water Res.* **2018**, *136*, 84–94. [CrossRef] [PubMed]
15. Murphy, K.R.; Stedmon, C.A.; Graeber, D.; Bro, R. Fluorescence Spectroscopy and Multi-Way Techniques. PARAFAC. *Anal. Methods* **2013**, *5*, 6557. [CrossRef]
16. Sciscenko, I.; Arques, A.; Micó, P.; Mora, M.; García-Ballesteros, S. Emerging Applications of EEM-PARAFAC for Water Treatment: A Concise Review. *Chem. Eng. J. Adv.* **2022**, *10*, 100286. [CrossRef]
17. Yang, L.; Hur, J.; Zhuang, W. Occurrence and Behaviors of Fluorescence EEM-PARAFAC Components in Drinking Water and Wastewater Treatment Systems and Their Applications: A Review. *Environ. Sci. Pollut. Res.* **2015**, *22*, 6500–6510. [CrossRef] [PubMed]
18. Wünsch, U.J.; Murphy, K. A Simple Method to Isolate Fluorescence Spectra from Small Dissolved Organic Matter Datasets. *Water Res.* **2021**, *19*, 116730. [CrossRef]
19. Nurhayati, M.; You, Y.; Park, J.; Lee, B.J.; Kang, H.G.; Lee, S. Artificial Neural Network Implementation for Dissolved Organic Carbon Quantification Using Fluorescence Intensity as a Predictor in Wastewater Treatment Plants. *Chemosphere* **2023**, *335*, 139032. [CrossRef]
20. Wells, M.J.M.; Funk, D.; Mullins, G.A.; Bell, K.Y. Application of a Fluorescence EEM-PARAFAC Model for Direct and Indirect Potable Water Reuse Monitoring: Multi-Stage Ozone–Biofiltration without Reverse Osmosis at Gwinnett County, Georgia, USA. *Sci. Total Environ.* **2023**, *886*, 163937. [CrossRef]
21. Yang, Y.Z.; Peleato, N.M.; Legge, R.L.; Andrews, R.C. Towards Real-Time Detection of Wastewater in Surface Waters Using Fluorescence Spectroscopy. *J. Environ. Sci.* **2019**, *86*, 195–202. [CrossRef]
22. Xiao, Y.; Ma, S.; Yang, S.; He, H.; He, X.; Li, C.; Feng, Y.; Xu, B.; Tang, Y. Using Machine Learning to Trace the Pollution Sources of Disinfection By-Products Precursors Compared to Receptor Models. *Sci. Total Environ.* **2024**, *914*, 169671. [CrossRef]

23. Cuss, C.W.; McConnell, S.M.; Guéguen, C. Combining Parallel Factor Analysis and Machine Learning for the Classification of Dissolved Organic Matter According to Source Using Fluorescence Signatures. *Chemosphere* **2016**, *155*, 283–291. [CrossRef] [PubMed]
24. Paradina-Fernández, L.; Wünsch, U.; Bro, R.; Murphy, K. Direct Measurement of Organic Micropollutants in Water and Wastewater Using Fluorescence Spectroscopy. *ACS ES T Water* **2023**, *3*, 3905–3915. [CrossRef]
25. Sciscenko, I.; García-Negueroles, P.; Amat, A.M.; Oller, I.; Escudero-Oñate, C.; Ferrando-Climent, L.; Arques, A. Use of Fluorescence Spectroscopy and Chemometrics to Visualise Fluoroquinolones Photodegradation Major Trends: A Confirmation Study with Mass Spectrometry. *Molecules* **2023**, *28*, 777. [CrossRef]
26. Sciscenko, I.; Mora, M.; Micó, P.; Escudero-Oñate, C.; Oller, I.; Arques, A. EEM-PARAFAC as a Convenient Methodology to Study Fluorescent Emerging Pollutants Degradation: (Fluoro)Quinolones Oxidation in Different Water Matrices. *Sci. Total Environ.* **2022**, *852*, 158338. [CrossRef] [PubMed]
27. Sciscenko, I.; Garcia-Ballesteros, S.; Sabater, C.; Castillo, M.A.; Escudero-Oñate, C.; Oller, I.; Arques, A. Monitoring Photolysis and (Solar Photo)-Fenton of Enrofloxacin by a Methodology Involving EEM-PARAFAC and Bioassays: Role of PH and Water Matrix. *Sci. Total Environ.* **2020**, *719*, 137331. [CrossRef]
28. McKnight, D.M.; Boyer, E.W.; Westerhoff, P.K.; Doran, P.T.; Kulbe, T.; Andersen, D.T. Spectrofluorometric Characterization of Dissolved Organic Matter for Indication of Precursor Organic Material and Aromaticity. *Limnol. Oceanogr.* **2001**, *46*, 38–48. [CrossRef]
29. Huguet, A.; Vacher, L.; Relexans, S.; Saubusse, S.; Froidefond, J.M.; Parlanti, E. Properties of Fluorescent Dissolved Organic Matter in the Gironde Estuary. *Org. Geochem.* **2009**, *40*, 706–719. [CrossRef]
30. Zsolnay, A.; Baigar, E.; Jimenez, M.; Steinweg, B.; Saccomandi, F. Differentiating with Fluorescence Spectroscopy the Sources of Dissolved Organic Matter in Soils Subjected to Drying. *Chemosphere* **1999**, *38*, 45–50. [CrossRef]
31. Micó, P.; García-Ballesteros, S.; Mora, M.; Vicente, R.; Amat, A.M.; Arques, A. EEMlab: A Graphical User-Friendly Interface for Fluorimetry Experiments Based on the DrEEM Toolbox. *Chemom. Intell. Lab. Syst.* **2019**, *188*, 6–13. [CrossRef]
32. Lawaetz, A.J.; Stedmon, C.A. Fluorescence Intensity Calibration Using the Raman Scatter Peak of Water. *Appl. Spectrosc.* **2009**, *63*, 936–940. [CrossRef]
33. Sciscenko, I.; Thị Mỹ Hắng, H.; Escudero-Oñate, C.; Oller, I.; Arques, A. Fluorescence Spectroscopy and Chemometrics: A Simple and Easy Way for the Monitoring of Fluoroquinolone Mixture Degradation. *ACS Omega* **2021**, *6*, 4663–4671. [CrossRef]
34. Bro, R.; Kiers, H.A.L. A New Efficient Method for Determining the Number of Components in PARAFAC Models. *J. Chemom.* **2003**, *17*, 274–286. [CrossRef]
35. Henderson, R.K.; Baker, A.; Murphy, K.R.; Hambly, A.; Stuetz, R.M.; Khan, S.J. Fluorescence as a Potential Monitoring Tool for Recycled Water Systems: A Review. *Water Res.* **2009**, *43*, 863–881. [CrossRef] [PubMed]
36. Murphy, K.R.; Hambly, A.; Singh, S.; Henderson, R.K.; Baker, A.; Stuetz, R.; Khan, S.J. Organic Matter Fluorescence in Municipal Water Recycling Schemes: Toward a Unified PARAFAC Model. *Environ. Sci. Technol.* **2011**, *45*, 2909–2916. [CrossRef]
37. Fox, B.G.; Thorn, R.M.S.; Anesio, A.M.; Reynolds, D.M. The in Situ Bacterial Production of Fluorescent Organic Matter; an Investigation at a Species Level. *Water Res.* **2017**, *125*, 350–359. [CrossRef] [PubMed]
38. Nowicki, S.; Lapworth, D.J.; Ward, J.S.T.; Thomson, P.; Charles, K. Tryptophan-like Fluorescence as a Measure of Microbial Contamination Risk in Groundwater. *Sci. Total Environ.* **2019**, *646*, 782–791. [CrossRef]
39. Yang, L.; Shin, H.S.; Hur, J. Estimating the Concentration and Biodegradability of Organic Matter in 22 Wastewater Treatment Plants Using Fluorescence Excitation Emission Matrices and Parallel Factor Analysis. *Sensors* **2014**, *14*, 1771–1786. [CrossRef]
40. Shutova, Y.; Baker, A.; Bridgeman, J.; Henderson, R.K. Spectroscopic Characterisation of Dissolved Organic Matter Changes in Drinking Water Treatment: From PARAFAC Analysis to Online Monitoring Wavelengths. *Water Res.* **2014**, *54*, 159–169. [CrossRef]
41. Gao, K.; Yang, H.; Liu, H.; Dong, B. Alleviating Ultrafiltration Membrane Fouling Caused by Effluent Organic Matter Using Pre-Ozonation: A Perspective of EEM and Molecular Weight Distribution. *Membranes* **2023**, *13*, 452. [CrossRef]
42. Deborde, M.; von Gunten, U. Reactions of Chlorine with Inorganic and Organic Compounds during Water Treatment-Kinetics and Mechanisms: A Critical Review. *Water Res.* **2008**, *42*, 13–51. [CrossRef] [PubMed]
43. Miklos, D.B.; Remy, C.; Jekel, M.; Linden, K.G.; Drewes, J.E.; Hübner, U. Evaluation of Advanced Oxidation Processes for Water and Wastewater Treatment—A Critical Review. *Water Res.* **2018**, *139*, 118–131. [CrossRef] [PubMed]